

# **Single-Phase Current-Source Rectifier Closed-Loop Control with Active Power Decoupling Based on LC Resonator Emulation**

**Yaser F. N. Ghazal**

Submitted to the  
Institute of Graduate Studies and Research  
in partial fulfillment of the requirements for the degree of

Master of Science  
in  
Electrical and Electronic Engineering

Eastern Mediterranean University  
February 2022  
Gazimağusa, North Cyprus

Approval of the Institute of Graduate Studies and Research

---

Prof. Dr. Ali Hakan Ulusoy  
Director

I certify that this thesis satisfies all the requirements as a thesis for the degree of Master of Science in Electrical and Electronic Engineering.

---

Assoc. Prof. Dr. Rasime Uygurođlu  
Chair, Department of Electrical and  
Electronic Engineering

We certify that we have read this thesis and that in our opinion it is fully adequate in scope and quality as a thesis for the degree of Master of Science in Electrical and Electronic Engineering.

---

Prof. Dr. Osman Kükre  
Supervisor

---

Examining Committee

1. Prof. Dr. Hasan Kömürçügil

---

2. Prof. Dr. Osman Kükre

---

3. Assoc. Prof. Dr. Samet Biricik

---

## ABSTRACT

AC-DC converters are power electronic systems which are used in a variety of industrial applications. These systems are better and more efficient than the regular AC-line commutated thyristor converters. The AC-DC converters can be regulated to draw sinusoidal currents from an AC source with variable power factor. Furthermore, they can produce smoother output voltages than the output voltages produced by the classical converters, especially in the three-phase usages.

Nevertheless, in single-phase usages the output voltage of a PWM converter has a naturally occurring second harmonic component, which requires the use of a large output capacitor for separating this component. But even when using a large capacitor (which raises the proportions and cost of this me of converter) it is still not possible to eliminate the second harmonic completely.

A better option for eliminating the second harmonic issue is to use an LC resonator that is modified or adjusted to eliminate this harmonic. This option can be easily applied in AC-DC converters of the current source type.

In this thesis, the LC resonator-based single-phase converter will be considered. The work will be based on an IEEE Transaction paper.

Firstly, the basic theory of this AC-DC converter will be revised, then the control strategy planned for eliminating the second harmonic component (which is based on active power decoupling) will be analyzed. Simulations on the single-phase current source converter will be done on Simulink. The simulations will be designed to assess

the performance of the planned control strategy. Possible failures of the control strategy will be acknowledged, and adjustments will be made accordingly.

**Keywords:** active power decoupling, LC Tank, ripple power, single-phase current source rectifier.

## ÖZ

AC-DC dönüştürücüler, çeşitli endüstriyel uygulamalarda kullanılan güç elektroniği sistemleridir. Bu sistemler, normal AC hattı komütasyonlu tristör dönüştürücülerden daha iyi ve daha verimlidir. AC-DC dönüştürücüler, değişken güç faktörlü bir AC kaynağından sinüzoidal akımlar çekmek için düzenlenebilir. Ayrıca özellikle üç fazlı kullanımlarda klasik dönüştürücülerin ürettiği çıkış gerilimlerinden daha düzgün çıkış gerilimleri üretebilirler.

Bununla birlikte, tek fazlı kullanımlarda, bir PWM dönüştürücünün çıkış voltajı, bu bileşeni ayırmak için büyük bir çıkış kapasitörünün kullanılmasını gerektiren, doğal olarak oluşan bir ikinci harmonik bileşene sahiptir. Ancak büyük bir kapasitör kullanıldığında bile (bu dönüştürücünün oranlarını ve maliyetini yükseltir) ikinci harmoniği tamamen ortadan kaldırmak hala mümkün değildir.

İkinci harmonik sorununu ortadan kaldırmak için daha iyi bir seçenek, bu harmoniği ortadan kaldırmak için değiştirilmiş veya ayarlanmış bir LC rezonatör kullanmaktır. Bu seçenek, mevcut kaynak tipindeki AC-DC dönüştürücülerde kolaylıkla uygulanabilir.

Bu tezde, LC rezonatör tabanlı tek fazlı dönüştürücü ele alınacaktır. Çalışma, bir IEEE İşlem belgesine dayanacaktır.

Öncelikle bu AC-DC dönüştürücünün temel teorisi gözden geçirilecek, ardından ikinci harmonik bileşenin (aktif güç ayrıştırmasına dayanan) ortadan kaldırılması için planlanan kontrol stratejisi analiz edilecektir. Tek fazlı akım kaynağı dönüştürücü

üzerinde simülasyonlar Simulink üzerinde yapılacaktır. Simülasyonlar, planlanan kontrol stratejisinin performansını değerlendirmek için tasarlanacaktır. Kontrol stratejisinin olası başarısızlıkları kabul edilecek ve buna göre ayarlamalar yapılacaktır.

**Anahtar Kelimeler:** aktif güç ayırma, LC rezonatör, dalgalı güç, tek fazlı akım kaynağı doğrultucu.

*To My Family*

# TABLE OF CONTENTS

ABSTRACT .....	iii
ÖZ .....	v
DEDICATION .....	vii
LIST OF TABLES .....	ix
LIST OF FIGURES .....	x
LIST OF SYMBOLS AND ABBREVIATIONS .....	xi
1 INTRODUCTION .....	1
2 LITERATURE REVIEW.....	4
3 SINGLE PHASE CURRENT RECTIFIER.....	8
3.1 Rectifier Circuit Passive Implementation .....	8
3.2 Proposed The Power Decoupling Control.....	12
3.3 Circuit Realization in Practical Terms .....	13
3.4 The Control Method.....	13
3.5 Simulation .....	15
4 DISCUSSION .....	20
5 SIMULATION RESULTS .....	22
6 CONCLUSION .....	29
REFERENCES.....	30



# LIST OF TABLES

Table 5.1: Input Parameters for Simulation .....	22
--	----

## LIST OF FIGURES

Figure 3.1: Single-Phase Current-Source Rectifier.....	8
Figure 3.2: Single-Phase –Current Source Rectifier with An LC Tank.....	10
Figure 3.3 (a) Asymmetric H-bridge circuit. (b) H-bridge circuit.....	10
Figure 3.4: Current Source Rectifier with Active Decoupling Circuit Converter Model .....	16
Figure 3.5: High-Frequency Bridge Rectifier Subsystem.....	16
Figure 3.6: Rectifier Controller.....	17
Figure 3.7: PWM Generating Block .....	17
Figure 3.8: Rectifier Control Loop.....	17
Figure 3.9:Asymmetric Bridge Converter.....	18
Figure 3.10: LC Emulator Control Loop .....	19
Figure 5.1: Line Grid Voltage $V_g$ and $I_{dc}$ Current.....	23
Figure 5.2: Capacitor $V_g$ Voltage and Current $I_g$ .....	23
Figure 5.2: The Output of Rectifier Control Loop.....	25
Figure 1: The step change in the load from 4.2 to 6 Ohms.....	23
Figure 5.4: The Grid Voltage vs the Grid Current .....	24
Figure 5.5: Duty Cycle $d_d, d_5, d_6$ .....	25
Figure 5.6 Fourier analysis for grid voltage $I_g$ .....	25
Figure 5.7: Current Source Rectifier Without Active Decoupling Circuit Converter Model .....	26
Figure 5.8: Line Grid Voltage $V_g$ and $I_{dc}$ Current.....	26
Figure 5.9: The Grid Voltage $V_g$ vs the Grid Current $I_g$ .....	27
Figure 5.10: Fourier analysis for Grid Voltage $\phi_g$ .....	27

## LIST OF SYMBOLS AND ABBREVIATIONS

CSC	Current Source Converter
$d_i$ & $d_d$	Duty Ratios
$f_g$	Input Frequency
$f_s$	Switching Frequency
$i_{rec}$	Chopping Current
$k_{p1}$ & $k_{i1}$	Controller Parameters
$k_r$	Adjustable Resonant Gain The Duty Ratio Used For Which
	$d_i (i = 1, 2, \dots, 6)$
$L_{dc}$	Dc Inductance
$L_g$	Input Filter Inductance
$\tilde{p}$	Ac Component $(\frac{T_k G_{amp} \omega_e r'}{0})$
$p$	Dc Component $(\frac{V_m I_m}{2})$
$R_L$	Load Resistance
$v_g$	Input Grid Voltage
$\omega_r$	Resonant Frequency
VSC	Voltage Source Converter

# Chapter 1

## INTRODUCTION

In the present technological world, the use of power electronics is increasing in the industry as well as in household/commercial applications. The development of power electronics technology plays a vital role in more applications, and these applications involve single phase power systems. By considering the single-phase power, most of the distributed energy such as energy coming from the solar cells, fuel cells and from many more energy sources are transferred to the grid utility using the concept of inverters (single phase grid connected) (Singh, 2004; Cha, 2015). Single-phase power is also used by residential power supplies, industrial as well as the system of lightning (Yilmaz, 2012). Besides, this power has some disadvantages in terms of performance which lead to reduction of the reliability of the system as well as the performance in terms of different parameter disturbances (Li S. , 2015).

To overcome these challenges, the best way is to use active as well as passive methods. The standpoints of the hardware come from the passive method. To apply this method, it is categorized in two types. We can either use LC resonant filters or the dc-link inductance or capacitance (Wang R. , 2010), respectively. The main issue in this method is the economic cost due to the high volume as well as weight of the devices. On the other hand, it is very easy to implement, therefore, it can be suggested to use this method. Moreover, the active method buffers the ripple power while using small inductors and capacitors to allow current as well as voltage fluctuations.

Inverters can be used as two-stage inverters which are single phase and contains front end dc-dc converter and inverters can also be downstream dc-ac inverter, respectively. The main issue considered by different researchers is the maintenance of the source current (SC) free from the second harmonic current ripple as well as the dynamic response of ac current quality, and dc-link voltage conflict are also under consideration and discussed in (Ksiazek, 2013;Kwon, 2008). The pros of the proposed method are that there is no involvement of the extra equipment of the circuit to be connected. On the other hand, there are also cons of this method, in that it is the less applied of the method because it is not proper for single phase converters.

When using this method, the voltage stress increases due to the second order ripple voltage super imposition on the DC bus. Therefore, another active method was adopted by adding an extra decoupling circuit. This method is analyzed (Sun, Review of active power decoupling topologies in single-phase systems, 2015) more than the previous method due to the variety of parallel as well as series decoupling circuits (Krein, 2012;Wang, 2013) which are used in order to balance the power difference between the load and source.

It has been found that resonant tanks result in sensitivity to line voltage distortion and the ability to generate realistic line-side inductances. To eliminate this instability, a possible solution using current feedback is proposed. Additionally, the added LC tank circuit increases system order and affects DC dynamics. To improve the system performance, we considered a resonant LC filter and proposed partial-state feedback control. The overall value of the passive component is reduced by using an LC resonator, but the size is still large due to the low resonant frequency. Another disadvantage is that the resonant frequency changes as the LC parameters drift. This

causes residual ripple power to flow on the DC link side and degrades the decoupling performance. This thesis proposes an active power decoupling control method for single-phase CSC. An electrical circuit is inserted into the DC link to simulate the external voltage characteristics of the parallel LC loop circuit. The existing literature on the proposed decoupling circuits are studied, and the simulation results are highlighted from different sources in the literature. Moreover, the challenges from the existing literature are also considered and discussed in detail as follows in the next chapter.

## Chapter 2

### LITERATURE REVIEW

Plenty of work is already done in this phenomenal research area. Some of the existing literatures are discussed in detail in the following paragraphs.

Single-phase power converters are generally suitable for low-power areas for example industrial and residential power supplies. (Singh, A review of single-phase improved power quality AC-DC converters, 2003). To validate and overcome the deficiency, active decoupling method is originated and used. In this method, the passive additional components store the ripple energy. Furthermore, the proposed methods are divided into two different categories as dependent and independent active decoupling methods (Sun, 2015; Bush, 2009). Previously, it was half bridge and full bridge decoupling circuits. Power semiconductor switches provide benefits to active decoupling approaches, which lead to reliable cost. This is the reason to install semiconductor devices between the original and decoupling circuits, respectively. The proposed decoupling circuit results in two actions, the inversion/rectification as well as the power decoupling. Therefore, in research articles (Li H. , Active power decoupling for high-power single-phase PWM rectifiers, 2012), (Vitorino, Single-phase power compensation in a current source converter, 2013),

it is stated that the power of semiconducting material devices of the proposed decoupling method can be partially minimized. Furthermore, authors in (Vitorino,

Compensation of DC-link oscillation in single-phase-to-single-phase VSC/CSC and power density comparison, 2013), shared a whole bridge arm between the original and decoupling circuit and is known as horizontal multiplexing method. Similarly, a vertical multiplexing method is presented in (Hartmann, 2014) by sharing two lower/upper switches of an original rectifier/inverter. Besides, an AC filter which is the combination of two identical capacitors is used in order to buffer ripple energy (Correa, 2013), in this case, the configuration of the circuits was the H-bridge differential circuit. The solutions of decoupling can be categorized in two categories. In the first category, for both filtering and energy storage, the decoupling capacitors are used and presented by (Serban, 2015; Tang, 2014). In the second, for energy storage only, the decoupling capacitors are adopted which was discussed by (Qi, 2014) (Ming, 2015). Previously, the buck differential inverter (Zhu G. , 2012) and boost differential converter (Zhu G. , 2014) circuits were used. Both the circuits reduce the ripple power by controlling the common mode voltage at the output of the capacitor filter. While considering the already existing active decoupling methods, only voltage source converters are under consideration, and the main focus is on the voltage source converters. There are solutions for current source converters, but they are few, which are presented by (Bush, A single-phase current source solar inverter with reduced-size DC link, 2009), respectively. Furthermore, diodes and switches are needed for decoupling solutions as well. The conduction losses also appear due to the flow of DC-link current in half of the decoupling circuit semiconductor devices (Han, Single-phase current source converter with power decoupling capability using a series-connected active buffer, 2015).



The LC resonator can be used to achieve constant DC-link current. To block the ripple power, the resonator should be tuned to 100 Hz. Due to the requirement of large passive components in the proposed method (using an LC resonator), the reliability and power density can be degraded. Therefore, in article (Liu, 2020), the emulation of LC resonator output voltage characteristics is under discussion. Moreover, with the usage of an LC resonator, decoupling function is achieved. This study also avoids the parameter drifts of bulky passive components as well. Simulation results show that the proposed model is efficient and validated by building a prototype. Furthermore, research study based on decoupling is presented by (Chaudhary, 2012). In this study, the voltage of grid and decoupling capacitor are considered as series combination which are limiting the operational range (viable) of the dc-link voltage. Moreover, the decoupling capacitor was linked to the isolation transformer center tap as presented in (Qi, 2014). According to the proposed study, the proposed design makes the transformer design more complex and maximizes the current of the transformer connected.

The study proposed on active methods are discussed by (Qi, 2014; Serban, 2015). According to the authors, the active methods share the switches entirely as well as partially. The switches may be bridge arm switches by making a bridge as discussed in the previous study and it can also be the lower or upper two switches which are considered in the study (Li H. , Active power decoupling for high-power single-phase PWM rectifiers, 2013). In order to reduce the voltage utility ratio, it will lead to reduce the number of switches used in the design. It is very effective, because the increase in the number of switches increases the complexity of the circuit as well as the voltage stress (Cao, 2014; Cai, 2014). The circuits considered by (Han, Single-phase current

source converter with power decoupling capability using a series-connected active buffer, 2015), (Bush, A single-phase current source solar inverter with reduced-size DC link, 2009), (Vitorino, Single-phase power compensation in a current source converter, 2013), still required additional two switches for operation as well as two diodes are required. Furthermore, in the study (Han, Single-phase current source converter with power decoupling capability using a series-connected active buffer, 2015), an open loop control decoupling circuit is presented where the control strategy was followed by taking the decoupling capacitor voltage as a reference. The simulation results in the proposed study show that the decoupling performance in terms of efficiency is very difficult to achieve by using such a strategy, because in this strategy, the system faced some unknown disturbances in terms of grid harmonics and parameters drifts, respectively.

By motivation from the existing literature, in this study, we adopt a technique for the given problem to overcome the challenges in the existing literature in order to make the proposed circuit efficient in all prospects by considering different parameters. The proposed methodology of the study is discussed in detail in the following chapters.

## Chapter 3

### SINGLE PHASE CURRENT RECTIFIER

In this chapter we will describe the steps taken to design a single-phase LC Resonator that will be used for industrial applications. In this section we will explain the analysis, design, implementation, testing and evaluation of our system. There are multiple tasks we need to consider designing this system.

The planning process for the single-phase LC Resonator:

- 1- Rectifier circuit passive implementation.
1. Proposed power decoupling control.
2. Circuit realization in practical terms.
3. The Control Method.
4. Simulation.

#### 3.1 Rectifier Circuit Passive Implementation

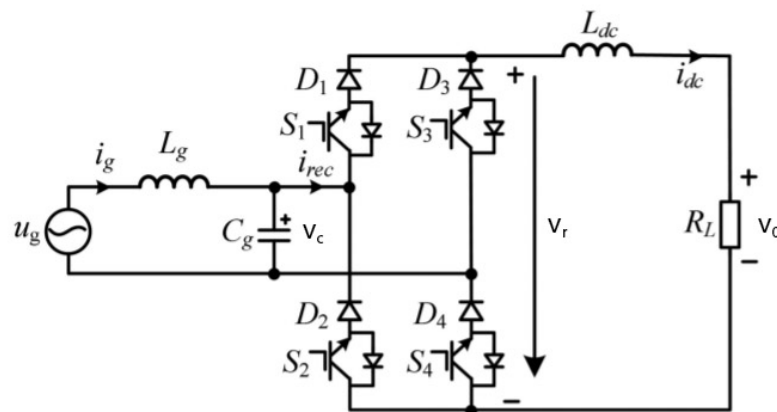


Figure:3.1 Single-phase Current-source Rectifier

Figure 3.1 illustrates the topology of the single-phase PWM rectifier circuit of the current source type. Capacitor  $C_g$  and inductor  $L_g$  on the AC side are configured as LC at a low-pass filter, to help convert  $i_{rec}$  chopping current to a sinewave.  $L_{dc}$  on the dc side acts as a smoothing filter and  $R_L$  indicates the load impedance.

Taking into consideration unity input power factor, the input current and voltage are given in equation (1) as:

$$\begin{aligned} i_g &= I_m \cos(\omega_g t) \\ u_g &= V_m \cos(\omega_g t) \end{aligned} \quad (1)$$

where  $\omega_g = 2\pi f$  is the grid angular frequency, and  $V_m$ ,  $I_m$  are the amplitudes of  $v_m$  and  $i_m$ .

Single-phase rectifiers with current sources have built-in ripple power at twice the mains frequency. Another way to achieve a constant DC current is to use a 100Hz LC resonator to suppress ripple component. However, this technology requires the use of large passive components, which reduces power density and reliability.

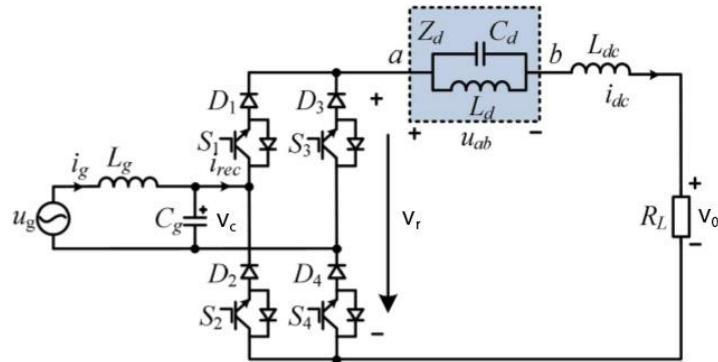


Figure 3.2: Single Phase Current Source Rectifier with an LC tank.

Figure 3.2 shows a parallel LC resonator, with the resonant frequency is set to twice the grid frequency ( $\omega = 2\omega_g$ ), is another possible solution, as illustrated in Figure 3.2.

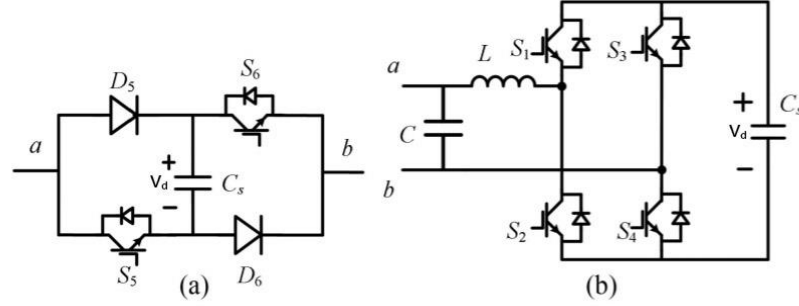


Figure 3.3: (a) Asymmetric H-bridge Circuit. (b) H-bridge Circuit.

In Figure 3.3 The emulator shown in (a) contains only one capacitor and two active switches, which can reduce the volume and the control complexity of the system. Therefore, it is adopted to verify the effectiveness of the proposed control method. When switches S5 and S6 are both turned OFF, the terminal output voltage  $v_{ab}$  is equal to  $v_d$ ; when switches S5 and S6 are both turned ON,  $v_{ab}$  is equal to  $-v_d$ ; while only one switch is turned ON,  $v_{ab}$  becomes zero. These three voltage levels are used to synthesize the expected voltage  $v_{ab}^*$ .

The Dc side of the dynamic differential equation is set as follow:

$$L_{dc} \frac{di_{dc}}{dt} = \frac{V_m I_m}{2i_{dc}} + \frac{V_m I_m}{2i_{dc}} \cos(2\omega_g t) - i_{dc} R_L \quad (2)$$

Let:

$$V_m I_m = p$$

$$I_{dc} = i$$

$$\omega_g = q$$

$$R_L = R$$

$$L_{dc} = l$$

$$l \frac{di}{dt} = \frac{p}{2i} + \frac{p \cos(2qt)}{2i} - iR \quad (3)$$

$$l \frac{di}{dt} + iR = \frac{p}{2i} + \frac{p \cos(2qt)}{2i} \quad (4)$$

We multiply by  $2i$

$$2iL \frac{di}{dt} + 2i^2R = p + p \cos(2qt) \quad (5)$$

Let:

$$y = i^2 \quad y' = 2i \frac{di}{dt}$$

$$y' + \frac{2Ry}{l} = \frac{p}{l} + \frac{p \cos(2qt)}{l} \quad (6)$$

$$\text{Solution :} \quad i^2 = \frac{p}{2R} + \frac{p(ql \sin(2qt) + R \cos(2qt))}{2(R^2 + q^2l^2)} + C^{-e^{-2Rt/l}} \quad (7)$$

To find C let us substitute C the initial conditions in the general solution:

$$y^2 = \frac{pql \sin(2qt)}{2R^2 + 2q^2l^2} + \frac{pR \cos(2qt)}{2R^2 + 2q^2l^2} + C^{-e^{-2Rt/l}} + \frac{p}{2R} \quad (8)$$

$$\begin{cases} x=0 \\ y=0 \end{cases} \rightarrow 0 = \frac{pR}{2R^2 + 2q^2l^2} + \frac{p}{2R} + C \quad (9)$$

$$C = \frac{2pR^2 + pq^2l^2}{2R^3 + 2q^2l^2R} \quad (10)$$

$$y^2 = \frac{pql \sin(2qt)}{2R^2 + 2q^2l^2} + \frac{pR \cos(2qt)}{2R^2 + 2q^2l^2} - \frac{2pR^2 + 2q^2l^2}{(2R^3 + 2q^2l^2R)e^{\frac{2Rt}{l}}} + \frac{p}{2R} \quad (11)$$

$$i^2 = \left( \frac{V_m I_m \omega_g L \sin(2\omega_g t) + V_m I_m R \cos(2\omega_g t)}{2R^2 + 2\omega_g^2 L^2} \right) - \left( \frac{2V_m I_m R^2 + V_m I_m \omega_g^2 L^2}{2(R^3 + \omega_g^2 t^2 R)e^{\frac{2Rt}{L}}} \right) + \left( \frac{V_m I_m}{2R} \right) \quad (12)$$

$$a = \frac{V_m I_m \omega_g L \sin(2\omega_g t) + V_m I_m R \cos(\omega_g t)}{2(R^2 + \omega_g^2 L^2)} + \frac{V_m I_m}{2R} \quad (13)$$

$$a = \frac{V_m I_m}{2} \left[ \frac{R\omega_g L \sin(2\omega_g t) + R \cos(2\omega_g t)}{R^2 + \omega_g^2 L^2} + \frac{1}{R} \right] = \frac{V_m I_m}{2} \left[ \frac{R\omega_g L \sin(2\omega_g t) + R^2 \cos(2\omega_g t) + R^2 + \omega_g^2 L^2}{R^2 + \omega_g^2 L^2} \right] \quad (14)$$

$$b = \frac{V_m I_m}{2} \left[ \frac{2R^2 + \omega_g^2 L^2}{R(R^2 + \omega_g^2 L^2)} e^{-\frac{2Rt}{L}} \right] \quad (15)$$

If we replace everything as mentioned above a and b will be

$$a = \frac{0.5V_m I_m [R_L^2 \cos(2\omega_g t) + R_L^2 + L_{dc}^2 \omega_g^2 + L_{dc} R_L \omega_g \sin(2\omega_g t)]}{R_L (R_L^2 + L_{dc}^2 \omega_g^2)}. \quad (16)$$

$$b = \frac{0.5V_m I_m (L_{dc}^2 \omega_g^2 + 2R_L^2) e^{-2R_L t / L_{dc}}}{R_L (R_L^2 + L_{dc}^2 \omega_g^2)}. \quad (17)$$

### 3.2 Proposed the Power Decoupling Control

The equation (5) shows the dynamics equations of  $v_{ab}$

$$v_{ab}(s) = \left( \frac{s/C_d}{s^2 + \frac{1}{L_d C_d}} \right) i_{dc}(s). \quad (18)$$

We deploy the same LC resonator to achieve similar results by employing another electric circuit in our design:

$$v_{ab}^* r(s) = \left( \frac{k_r s}{s^2 + \omega_r^2} \right) i_{dc}(s). \quad (19)$$

where  $\omega_r$  is the resonant frequency and  $k_r$  is the adjustable resonant gain.

The filter LC in general is used only for the ripple power to buffer it and it will not absorb any active power. To maintain the voltage of the capacitor we utilize a resistor to provide us voltage regulation.

$$v_{ab}(s) = \left( R_d + \frac{k_r s}{s^2 + \omega_r^2} \right) i_{dc}(s) \quad (20)$$

### 3.3 Circuit Realization in Practical Terms

There are many circuits available to emulate the LC filter operation. The output voltage  $v_{ab}$  at terminal is used to determine the reference voltage of circuit. When both switch in Figure(3.3) over Switch 5 and Switch 6 are OFF, the output power at the terminal is similar to  $v_d$ ; when both switch over Switch 5 and Switch 6 are turned ON,  $v_{ab}$  is the same to  $v_d$ , the only switch turned ON,  $v_{ab}$  becomes zero. The three-level

voltages that can be obtained through the control described above provide us the desired voltage  $v_{ab}$ .

Figure (3.2) shows the emulator which consist of components like capacitor and the two dynamic switches which help to make our model more efficient by reducing the volume and complexity of our system. Therefore, this circuit is chosen because it will suppress the second harmonic dc current efficiently.

### 3.4 The Control Method

The mathematical model of the as shown:

$$L_g \frac{di_g}{dt} = u_g - u_c \quad (21)$$

$$C_g \frac{du_c}{dt} = i_g - i_{rec} \quad (22)$$

$$L_{dc} \frac{di_{dc}}{dt} = v_r - v_{ab} - v_o \quad (23)$$

$$C_s \frac{du_d}{dt} = d_d i_{dc} \quad (24)$$

Here  $i_{rec} = d_r i_{dc}$  and  $v_{ab} = d_r v_c$  and  $d_d$  are given as follow:

$$\begin{cases} d_r = d_1 - d_2 \\ d_d = 1 - d_5 - d_6 \end{cases} \quad (25)$$

The regulator we have used is basically to provide us with the high-power factor and current to our load. Then we multiply both sides of equation (23) by the current  $i_{dc}$  and our equation becomes:

$$\frac{L_{dc}}{2} \frac{di_{dc}^2}{dt} = v_c i_{rec} - d_r v_d i_{dc} - v_o i_{dc} \quad (26)$$



where  $v_c i_{rec}$  is the input power,  $p \sim (-d_r v_d i_{dc})$  is the minor ripple, and  $P_0 (-v_0 i_{dc})$  is the output power. To Ignore the impacting of the low pass filter,  $v_c$  can be taken to be the same to  $v_g$ .

The reference input current is:

$$i_{rec}^* = I_m^* \cos(\omega_g t) \quad (27)$$

Equation (26) can be averaged over one period after substituting (27) into (26) obtaining:

$$L_{dc} \frac{\overline{(di_{dc}^2)}}{dt} = V_m I_m - 2P_0 \quad (28)$$

The average value of  $i_{dc}^2$  can be accomplished by using an average filter (MAF: moving average filter).

A proportional integral controller (PI) is then used to control the average value of  $i_{dc}$  the output of which is the reference for the current amplitude  $I_m^*$ .

$$I_m^* = \frac{1}{V_m} \{ [(i_{dc}^*)^2 - \overline{(i_{dc}^2)}] (k_{p1} + \frac{k_{i1}}{s}) + 2P_0 \}. \quad (29)$$

To control the behavior of the LC filter we must use asymmetric H-bridge controller.

The reference for the controlled voltage of the capacitor it consists of the two parts  $v_1$  and  $v_2$ . The component  $v_1$  is for the decoupling function and is obtained through multiplication of  $i_{dc}$  by the impedance of the LC tank circuit. Also,  $v_2$  is for stabilization of the capacitor voltage by the introduction of the virtual resistance  $R_d^*$ .

The designed  $R_d^*$  is the output of a PI regulator expressed as:

$$R_d^* = (v_d^* - \overline{v_d})(k_{p2} + \frac{k_{i2}}{s}) \quad (30)$$

Here  $k_{p2}$  and  $k_{i2}$  are the parameters of the PI controller,  $v_d^*$  is the reference of the capacitor voltage reference and  $\overline{v_d}$  obtained via an (MAF). When the control references  $i_{rec}^*$  and  $v_{ab}^*$  have being determined, the duty ratio  $d_i$ . and  $d_d$  could be clearly derived.

Here, the duty ratio for every switch is shown in equation (31) as:

$$\begin{aligned} d_1 &= \begin{cases} 1, & d_r > 0 \\ 0, & d_r \leq 0 \end{cases} & d_2 &= \begin{cases} 1-d_r, & d_r > 0 \\ -d_r, & d_r \leq 0 \end{cases} \\ d_3 &= \begin{cases} 0, & d_r > 0 \\ 1, & d_r \leq 0 \end{cases} & d_4 &= \begin{cases} d_r, & d_r > 0 \\ 1+d_r, & d_r \leq 0 \end{cases} \\ d_5 &= \begin{cases} 1-d_d, & d_d > 0 \\ 1, & d_d \leq 0 \end{cases} & d_6 &= \begin{cases} 0, & d_d > 0 \\ -d_d, & d_d \leq 0 \end{cases} \end{aligned} \quad (31)$$

It is worth nothing here that the criterion to achieve the active method decoupling is derived only from  $i_{dc}$ . This method for this current could be built into the sub-module of LC resonator emulator circuit.

### 3.5 Simulation

As a basis for simulating the operation of the proposed AC-DC converter, circuits and controllers from the source article were used. For illustrating the difference between CSC with power factor correction and proposed converter, first results were obtained by simulating the model in Figures (3.4-3.10), which was created in Matlab-Simulink by using the Simscape toolbox.

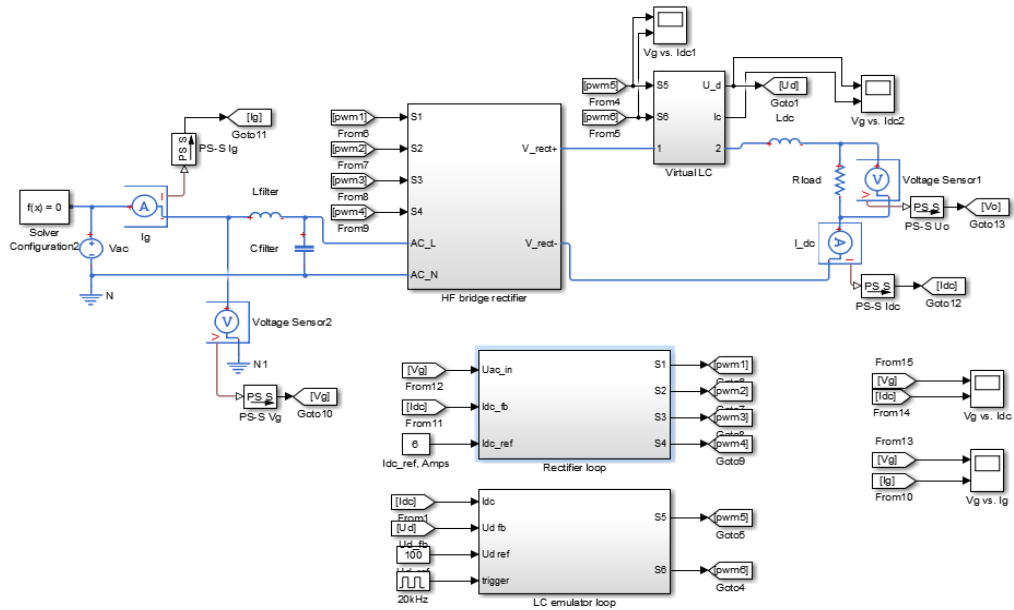


Figure 3.4: Current Source Rectifier with Active Decoupling Circuit Converter Model

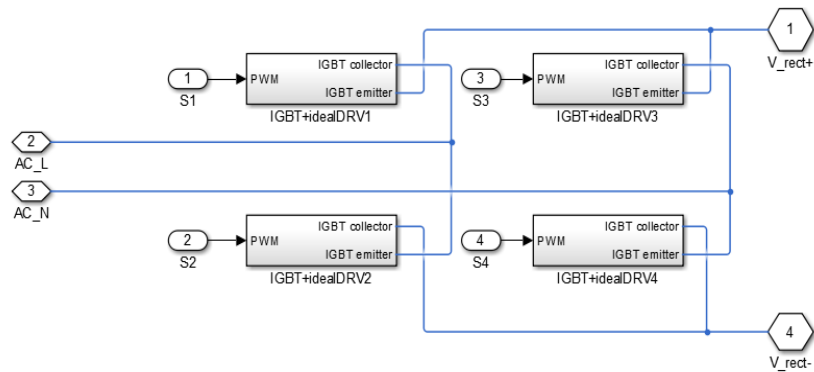


Figure 3.5: High-Frequency Bridge Rectifier Subsystem

HF bridge rectifier (Fig 3.4) is modelled using IGBT switches for simplification purposes. Processes and circuits, required for successful operation of such a converter in real life, are out of scope of this work, thus IGBT switch block is simplified as much as possible. Each ideal IGBT switch is composed of IGBT model driven by ideal controllable voltage source. Signals which control these voltage sources are generated by the rectifier controller in Fig. (5.3).

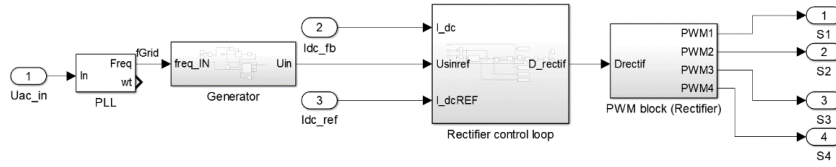


Figure 3.6: Rectifier Controller

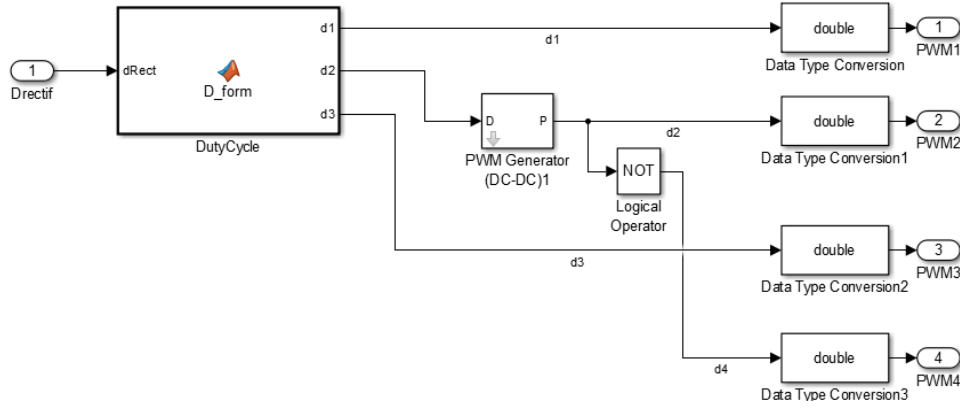


Figure 3.7: PWM Generating Block

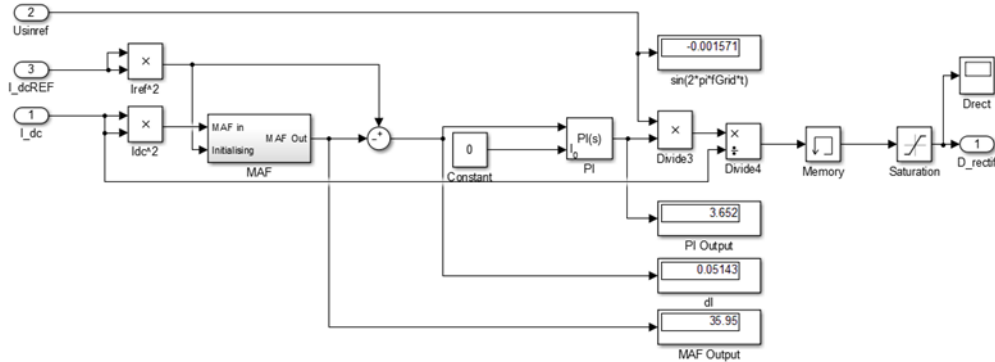


Figure 3.8: Rectifier Control Loop

Rectifier control loop implements the PI controller derived before:

$$I_m^* = \frac{1}{V_m} \{ [(i_{dc}^*)^2 - \overline{(i_{dc}^2)}] (k_{p1} + \frac{k_{i1}}{s}) + 2P_0 \}. \quad (32)$$

The main purpose of such a control loop is to regulate the output current by comparing it with its reference value. Moreover, grid voltage waveform is used to maximize power factor converter.

The circuit for active power decoupling is based on an asymmetric bridge (Fig.3.8) with capacitor acting as energy storage element. This capacitor is supplying/consuming energy to the output, thus ‘filtering’ the pulsating power created by the rectifier. Control method of such a circuit is based on emulating the LC-circuit, which is set to twice the grid frequency.

LC emulator control loop model (Fig. 3.7) implements usage of formula below:

$$v_{ab\_r}^*(s) = \left( \frac{k_r s}{s^2 + \omega_r^2} \right) i_{dc}(s). \quad R_d^* = (v_d^* - \overline{v_d}) \left( k_{p2} + \frac{k_{i2}}{s} \right) \quad (33)$$

Here  $k_{p2}$  and  $k_{i2}$  relates to the parameters of the regulator,  $v_d^*$  is the average value of the capacitor reference voltage also  $\overline{v_d}$  is obtained via MAF. After defining the control references  $i_{rec}^*$  and  $v_{ab}^*$ , the duty ratios  $d_i$  and  $d_d$  know how to be simply analyzed.

Furthermore, resistance emulating loop is added to satisfy energy storage requirement of the LC emulator circuit (energy stored in capacitor  $C_d$  should be more or equal to energy dissipated by the load between half-cycles of rectified current).

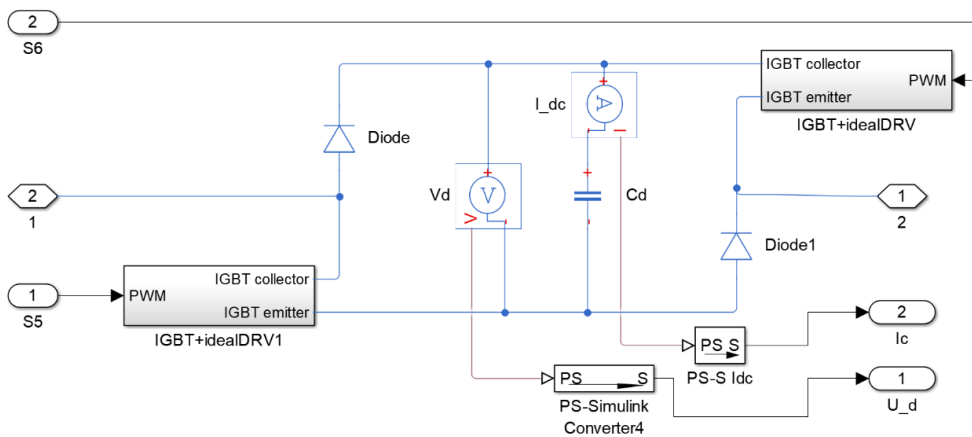


Figure 3.9: Asymmetric Bridge Converter

Control loop emulates LC resonant tank tuned to twice the grid frequency; also, an additional loop is added to ensure that the energy stored in the capacitor will be enough for decoupling operation. This control loop also outputs PWM signals for IGBT switches in the asymmetric bridge.

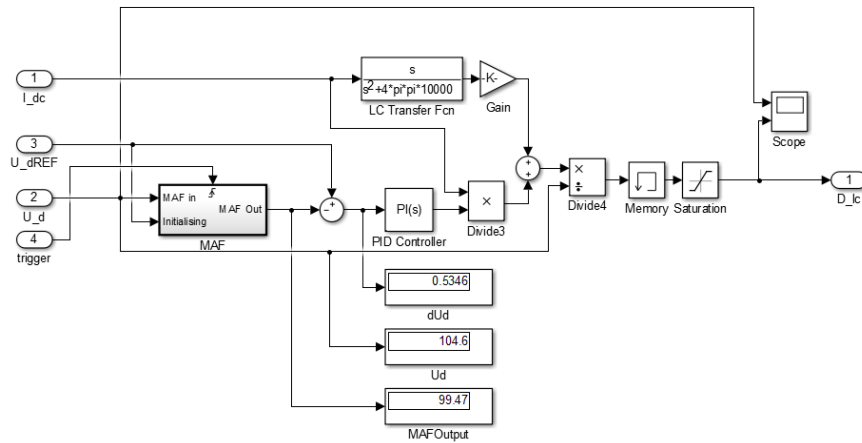


Figure 3.10: LC Emulator Control Loop

## Chapter 4

### DISCUSSION

In this chapter, we evaluated two techniques, which consist of the passive decoupling method and an existing technique for controlling active power decoupling. If a LC filter has a low resonant frequency, then the components are quite large. Consider the parameters  $L_d = 3.5 \text{ mH}$  and  $C_d = 1500 \text{ mF}$ , which are estimated to occupy  $300 \text{ cm}^3$ . However, with the proposed method, the actual volume is  $30 \text{ cm}^3$ .

On the other hand, the reliability of the suggested technique may decrease as number of semiconductor components used increases. The failure rate is evaluated by the use of the guide on estimating the reliability of electronic devices MIL- HDBK -217F.

These techniques are often divided into two categories, the first being Form A and the second being Form B. The control techniques are normally divided into two forms, referred to as Form A and Form B, depending on whether the controller allows Decoupling Modularity. In form A, both decoupling of the wave voltage then stabilization of the voltage of the decoupling capacitor are achieved by controlling the decoupling circuit and knowing the external information about current/voltage in the DC link. There is no need for any data to be transferred between the rectifier or inverter and the decoupling circuit. We have control techniques which are part of form B.

The majority of the existing control techniques are part of form B, such as round current compensation control, decoupling capacitor voltage tracking control for energy saving, and automatic power decoupling control. The design of this form of control is such that, a centralized control is selected to synchronize the inverter or the rectifier as well as the decoupling circuit operations. To reduce the number of components, we would need many decoupling circuits with switch multiplexing, where the switches perform the dual functions of power conversion and decoupling.

In this form of decoupling circuits, the techniques developed for control are all part of form B. In form A, the decoupling method is mainly used to emulate an actual module, such as an inductor, a capacitor, and a LC tank set to double the frequency of the line. Some techniques require hundred percent differential operation, and high frequency noise is amplified. A problem which is solved by sampling the capacitor current or the inductor voltage directly with an internal controller. Nonetheless, the capacitor current or inductor voltage is not smoothed, this may result in an increase in the complication of the required signal processing. Voltage/current sensing network as well as differential operation are circumvented in the proposed structure. Whereas only a capacitor voltage or inductor current used to mimic the required dynamic range. Hence, to consider a technique for controlling the proposed method of decoupling active power may be good, especially if a modular decoupling design is preferred



## Chapter 5

### SIMULATION RESULTS

To prove the effectiveness of the control strategy, we created a simulation model in the MATLAB environment. The simulation results of such a model are presented by comparing the input voltage and input current, and the input voltage and load current: Proposed circuit is using next given values (Table 1).

Table5.1: Input Parameters for Simulation

Symbol	Description	Value
$u_g$	Input grid voltage	110 V (rms)
$f_g$	Input frequency	50 Hz
$L_g$	Input filter inductance	0.6 mH
$C_g$	Input filter capacitance	20 $\mu$ F
$C_s$	Stored energy capacitance	100 $\mu$ F
$L_{dc}$	DC inductance	3.6 mH
$R_L$	Load resistance	6 $\Omega$
$f_s$	Switching frequency	20 KHZ
$K_{p1}$	proportional gain (PI)	0.3
$K_{i1}$	integral gain (PI)	15
$K_{p2}$	proportional gain (PID)	0.1
$K_{i2}$	integral gain (PID)	0.15

Simulation results are shown on graphs:  $V_g$  vs  $I_{dc}$  (Fig.5.1) and  $V_d$  vs  $I_d$  (Fig. 5.2).

These graphs show that proposed control methods for active power decoupling is satisfactory, given the nature of current source converter.

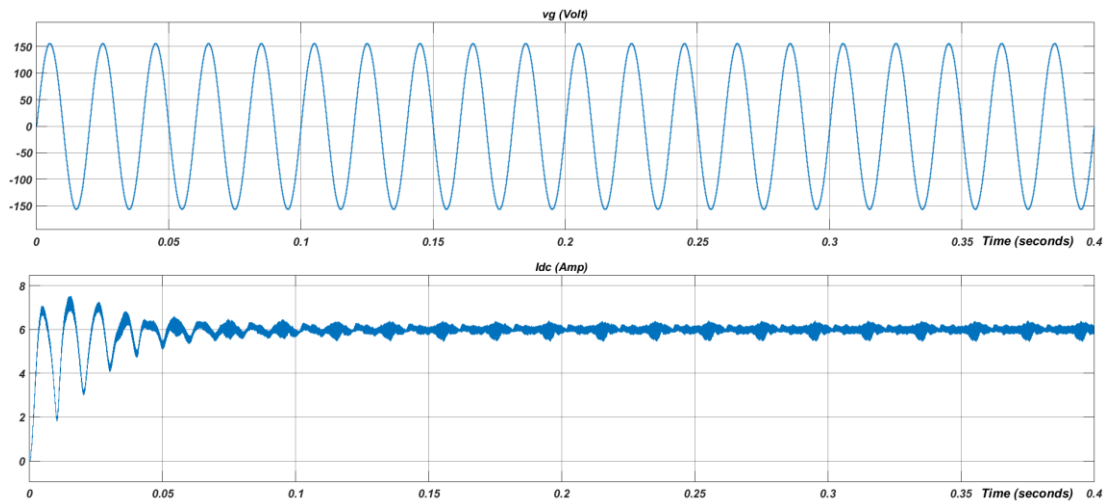


Figure5.1: Line Grid Voltage  $v_g$  and  $I_{dc}$  Current

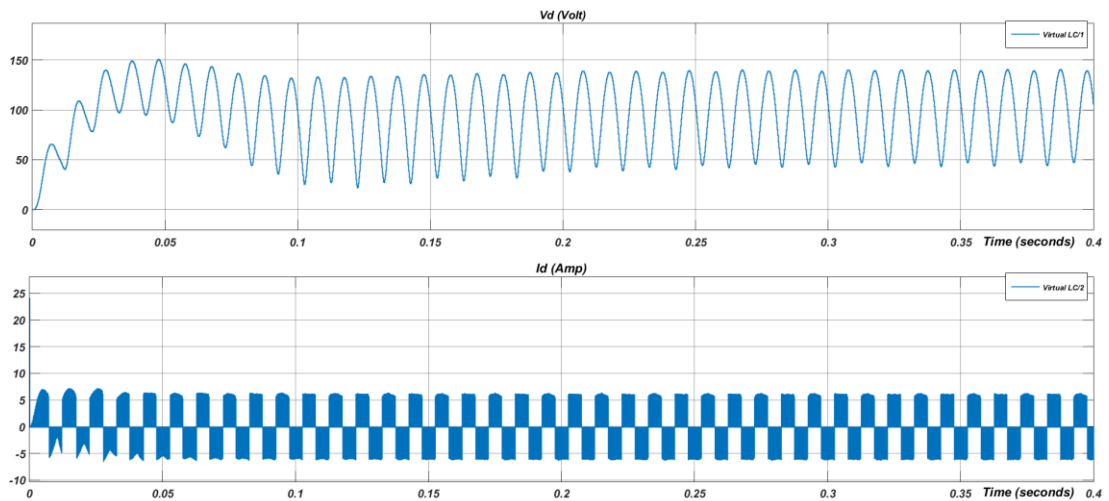


Figure 5.2: Capacitor  $V_d$  Voltage and Current  $I_d$

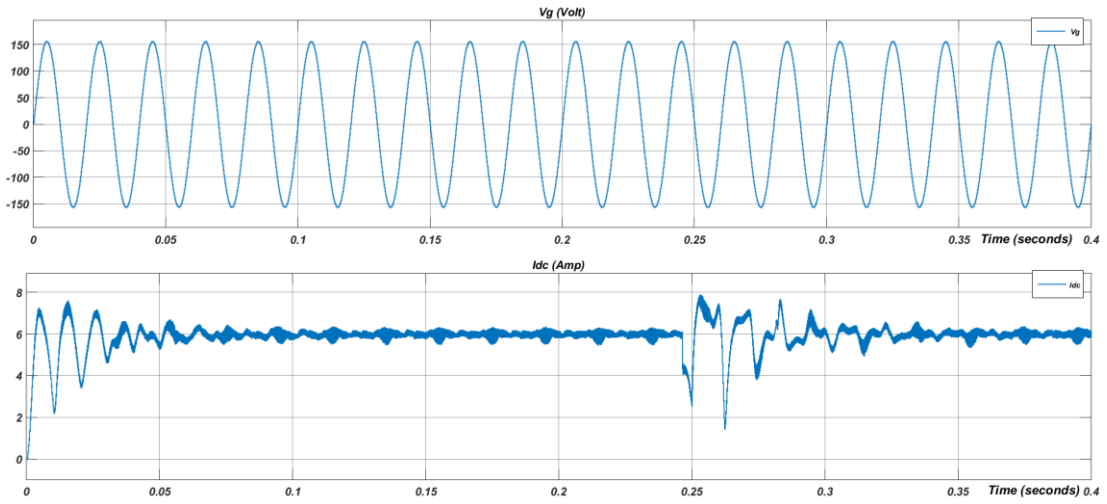


Figure 5.3: The step change in the load from 4.2 to 6 Ohms.

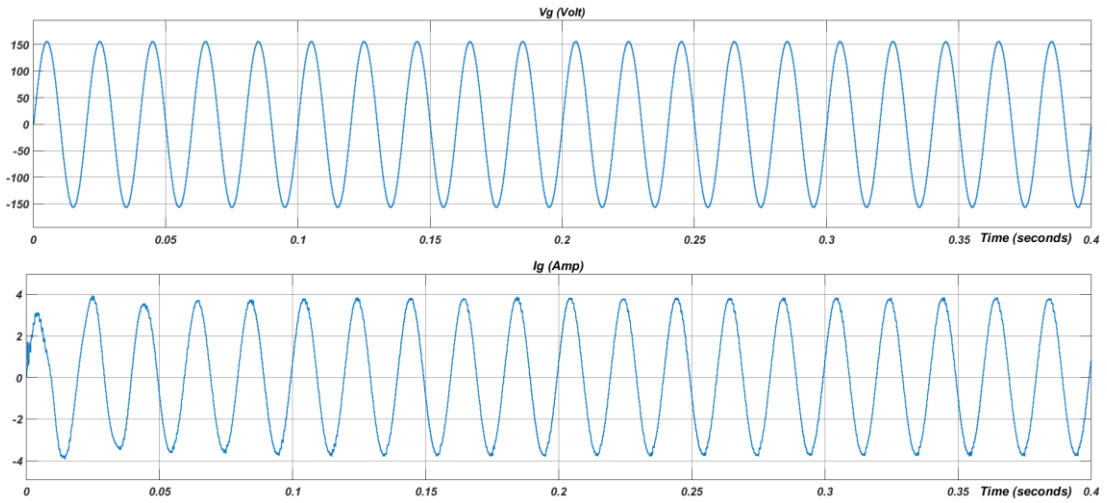


Figure 5.4: The Grid Voltage  $V_g$  vs the Grid Current  $I_g$

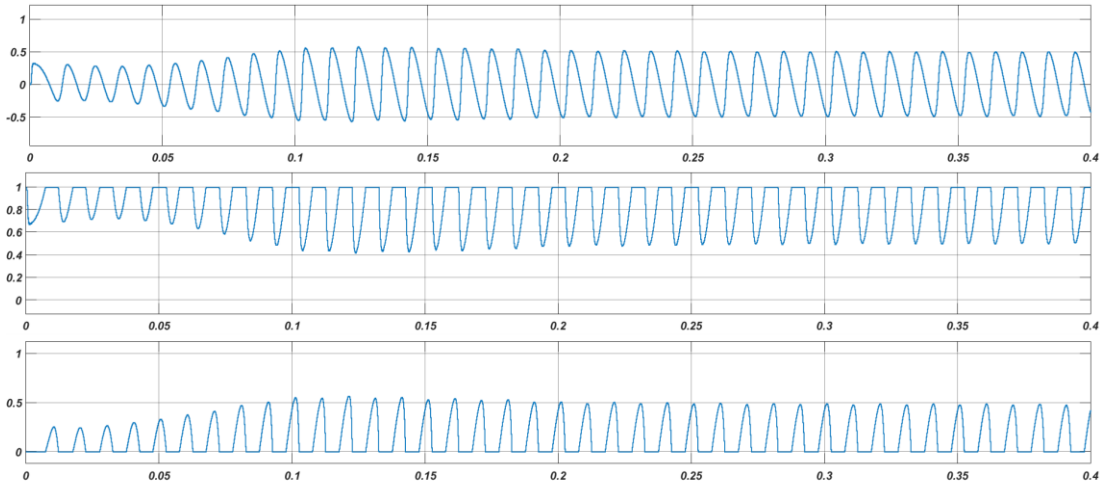


Figure:5.5 Duty cycle  $d_d, d_5, d_6$

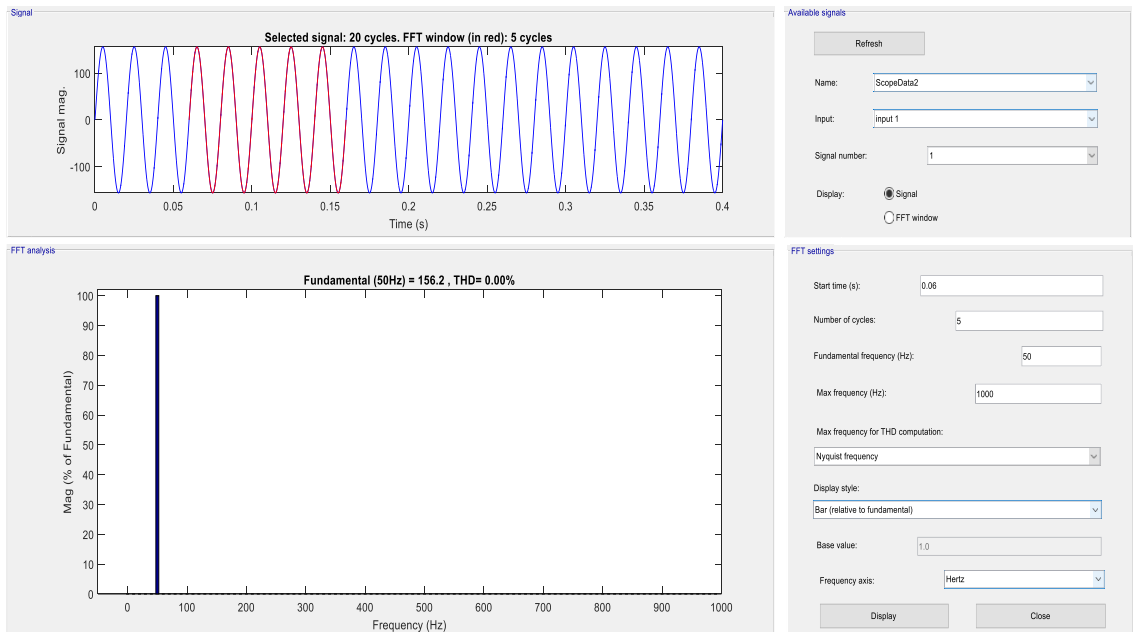


Figure5.6: Fourier analysis for grid voltage  $I$

To better appreciate the improvement brought by the active LC resonator, the circuit model without an LC emulator is constructed as shown in Figure (5.7).

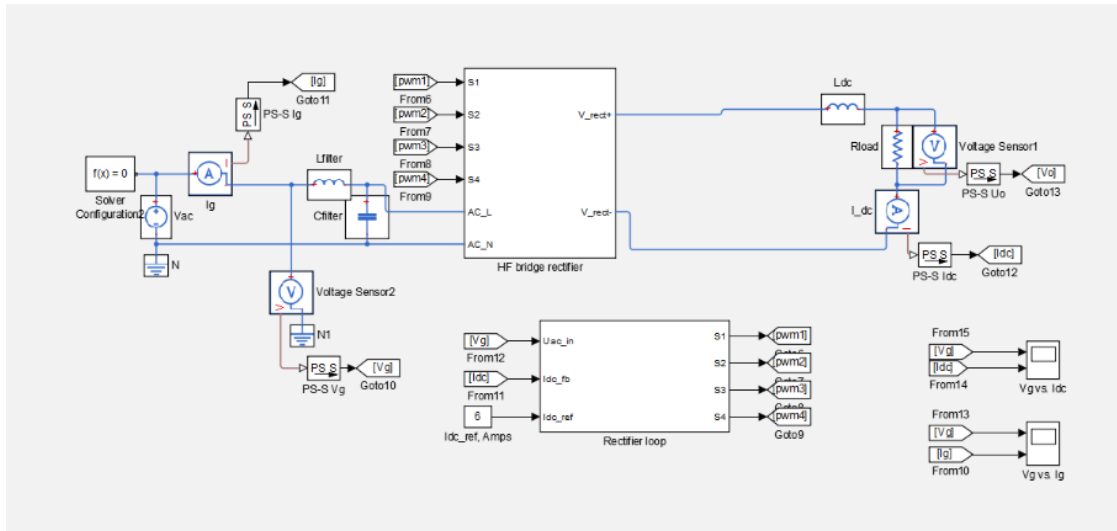


Figure 5.7: Current Source Rectifier Without Active Decoupling Circuit Converter Model

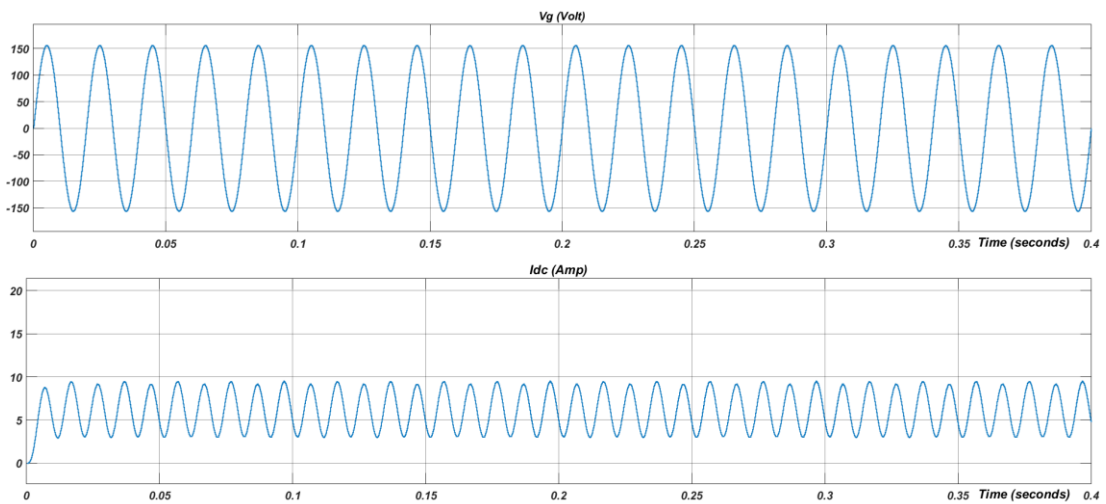


Figure 5.8: Line Grid Voltage  $V_g$  and  $I_{dc}$  Current

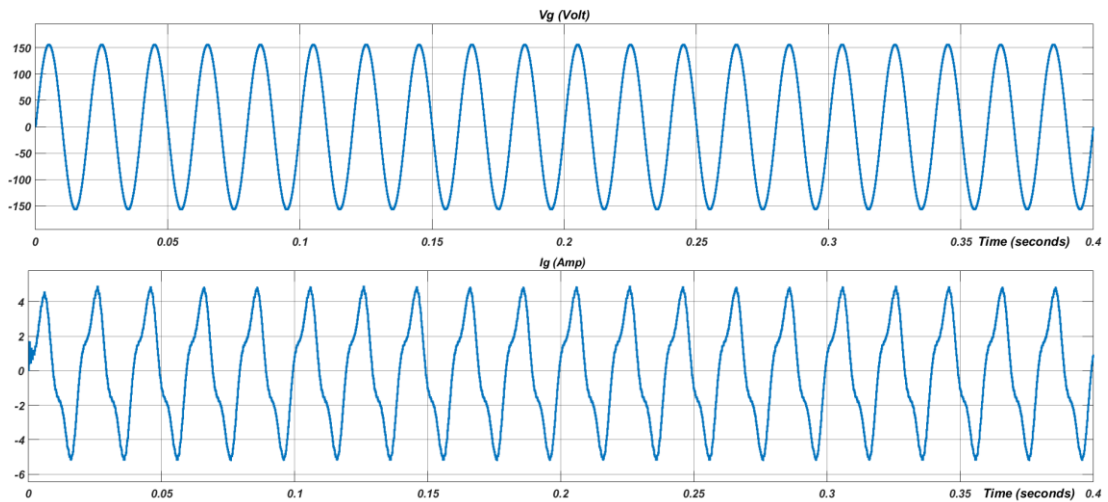


Figure 5.9: The Grid Voltage  $v_g$  vs the Grid Current  $i_g$

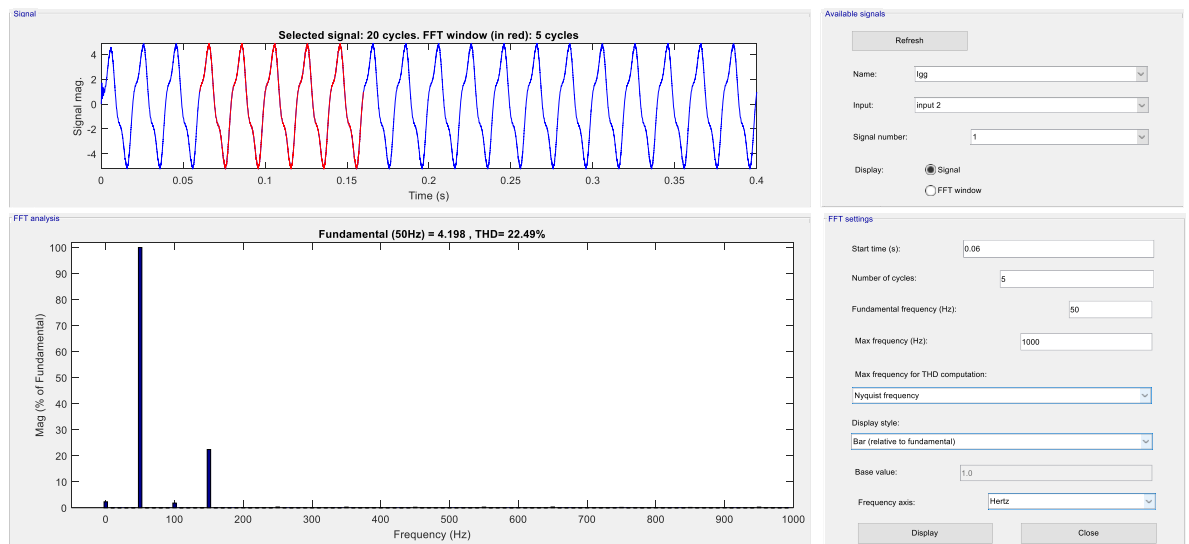


Figure 5.10: Fourier Analysis for Grid Voltage

However, during the process of developing this simulation model disadvantages and difficulties of such circuit were spotted:

- 1) While there is no specialized control IC for control loop available for real-life implementation, usage of digital signal processing ICs is required, which makes development more expensive.

- 2) Control loops used in this model are designed separately, while they both affect stability of the whole system. Any instability created by rectifier control loop will be seen by LC emulator control loop, which only drastically increases the complexity of designing such circuit.
  
- 3) Reaction to any step change of such circuit is not analyzed; it is estimated to increase design complexity even further.
  
- 4) While this model is simplified, further research of transient processes is required.
  
- 5) In Figure 5.3 the step change in load changed from 4.2 to 6 ohm. After we open the switch shown the slow because of the dynamic of the controller.

## **Chapter 6**

### **CONCLUSION**

In this thesis, the control capabilities were developed to achieve power decoupling in a single-phase power source rectifier. This was done through the use of an electrical circuit having similar characteristics as the LC tank, which buffers the double mains frequency of the output power perfectly. From the point of view of secondary voltage balance, the electrical circuit generated alternating voltage to stabilize for ripple factor and to cancel the resulting undulating voltage on the side of dc.



## REFERENCES

- C. R. Bush and B. Wang, (2009). A single-phase current source solar inverter with reduced-size DC link, IEEE Energy Conversion Congress and Exposition, , pp. 55, doi: 10.1109/ECCE.2009.5316285
- C. R. Bush and B. Wang, (2009)"A single-phase current source solar inverter with reduced-size DC link," IEEE Energy Conversion Congress and Exposition, , pp. 54, doi: 10.1109/ECCE.2009.5316285.
- Cai, Wen; Jiang, Ling; Liu, Bangyin; Duan, Shanxu; Zou, Changyue (2015). A Power Decoupling Method Based on Four-Switch Three-Port DC/DC/AC Converter in DC Microgrid. IEEE Transactions on Industry Applications,pp51, 336–343. doi:10.1109/tia.2014.2327162.
- X. Cao, Q. Zhong and W. Ming, (2015) "Ripple Eliminator to Smooth DC Bus Voltage and Reduce the Total Capacitance Required," in IEEE Transactions on Industrial Electronics, vol. 62, no. 4, pp.4 2224-2235, doi: 10.1109/TIE.2014.2353016.
- Cho, Yong-Won; Kim, Kyu-Tae; Cha, Woo-Jun; Kwon, Bong-Hwan; Lee, Sung-Ho (2015). Evaluation and analysis of transformer less photovoltaic inverter topology for efficiency improvement and reduction of leakage current. IET Power Electronics, 8(2), 255–267. doi:10.1049/iet-pel.2014.0401

P. Chaudhary and P. Sensarma, (2013) "Front-End Buck Rectifier With Reduced Filter Size and Single-Loop Control," in IEEE Transactions on Industrial Electronics, vol. 60, no. 10, pp. 4359-4368, Oct. 2013, doi: 10.1109/TIE.2012.2217724. Correa, M..

Sun, Yao; Su, Mei; Han, Hua; Xiong, Wenjing; Liu, Yonglu (2015). Single phase current source converter with power decoupling capability using a series-connected active buffer. IET Power Electronics, 8(5), 700-707. doi:10.1049/iet-pe.2014.0068

Sun, Yao; Su, Mei; Han, Hua; Xiong, Wenjing; Liu, Yonglu (2015). Single-phase current source converter with power decoupling capability using a series-connected active buffer. IET Power Electronics, 8(5), 700-707. doi:10.1049/iet-pe.2014.0068

M. A. Vitorino, L. V. Hartmann, D. A. Fernandes, E. L. Silva and M. B. R. Corrêa, (2014) "Single-phase current source converter with new modulation approach and power decoupling," IEEE Applied Power Electronics Conference and Exposition APEC 2014, 2014, pp. 2200-2207, doi: 10.1109/APEC.2014.6803610.

P. T. Krein, R. S. Balog and M. Mirjafari, (2012) "Minimum Energy and Capacitance Requirements for Single-Phase Inverters and Rectifiers Using a Ripple Port,"

in IEEE Transactions on Power Electronics, vol. 27, no. 11, pp. 4690-4698,  
doi: 10.1109/TPEL.2012.2186640.

P. F. Ksiazek and M. Ordonez, (2014)"Swinging Bus Technique for Ripple Current Elimination in Fuel Cell Power Conversion," in IEEE Transactions on Power Electronics, vol. 29, no. 1, pp. 170-178, Jan., doi: 10.1109/TPEL.2013.2251357.

J. Kwon, E. Kim, B. Kwon and K. Nam, (2009)"High-Efficiency Fuel Cell Power Conditioning System With Input Current Ripple Reduction," in IEEE Transactions on Industrial Electronics, vol. 56, no. 3, pp. 826-834,doi: 10.1109/TIE.2008.2004393

H. Li, K. Zhang, H. Zhao, S. Fan and J. Xiong, (2013)"Active Power Decoupling for High-Power Single-Phase PWM Rectifiers," in IEEE Transactions on Power Electronics, vol. 28, no. 3, pp. 1308-1319, doi: 10.1109/TPEL.2012.2208764.

H. Li, K. Zhang, H. Zhao, S. Fan and J. Xiong, (2013)"Active Power Decoupling for High-Power Single-Phase PWM Rectifiers," in IEEE Transactions on Power Electronics, vol. 28, no. 3, pp. 1308-1319, doi: 10.1109/TPEL.2012.2208764.

S. Li, S. -C. Tan, C. K. Lee, E. Waffenschmidt, S. Y. Hui and C. K. Tse, (2016)"A survey, classification, and critical review of light-emitting diode drivers," in IEEE Transactions on Power Electronics, vol. 31,no.2,pp.1503-1516,doi: 10.1109/TPEL.2015.2417563.

- Y. Liu, W. Zhang, J. Lin, M. Su and X. Liang, (2021)"Active Power Decoupling Control for Single-Phase Current Source Rectifier Based on Emulating LC Resonator," in IEEE Transactions on Industrial Electronics, vol. 68, no. 6, pp. 5460-5465, , doi: 10.1109/TIE.2020.2984981.
- W. -L. Ming, Q. -C. Zhong and X. Zhang, (2016)"A Single-Phase Four-Switch Rectifier With Significantly Reduced Capacitance," in IEEE Transactions on Power Electronics, vol. 31, no. 2, pp. 1618-1632, doi: 10.1109/TPEL.2015.2414425.
- W. Qi, H. Wang, X. Tan, G. Wang and K. D. T. Ngo, (2014) "A novel active power decoupling single-phase PWM rectifier topology," 2014 IEEE Applied Power Electronics Conference and Exposition - APEC, 2014, pp. 89-95, doi: 10.1109/APEC.2014.6803293.
- I. Serban (2015), "Power Decoupling Method for Single-Phase H-Bridge Inverters With No Additional Power Electronics," in IEEE Transactions on Industrial Electronics, vol. 62, no. 8, pp. 4805-4813, , doi: 10.1109/TIE.2015.2399274.
- I. Serban (2015), "Power Decoupling Method for Single-Phase H-Bridge Inverters With No Additional Power Electronics," in IEEE Transactions on Industrial Electronics, vol. 62, no. 8, pp. 4805-4813, , doi: 10.1109/TIE.2015.2399274.
- B. Singh, B. N. Singh, A. Chandra, K. Al-Haddad, A. Pandey and D. P. Kothari, (2003)"A review of single-phase improved power quality AC-DC converters,"

in IEEE Transactions on Industrial Electronics, vol. 50, no. 5, pp. 962-981,doi:  
10.1109/TIE.2003.817609.

B. Singh, B. N. Singh, A. Chandra, K. Al-Haddad, A. Pandey and D. P. Kothari,  
(2004)"A review of three-phase improved power quality AC-DC converters,"  
in IEEE Transactions on Industrial Electronics, vol. 51, no. 3, pp. 641-660, doi:  
10.1109/TIE.2004.825341.

Y. Sun, Y. Liu, M. Su, W. Xiong and J. Yang, (2015)"Review of Active Power  
Decoupling Topologies in Single-Phase Systems," in IEEE Transactions on  
Power Electronics, vol. 31, no. 7, pp. 4778-4794, doi:  
10.1109/TPEL.2015.2477882.

Y. Sun, Y. Liu, M. Su, W. Xiong and J. Yang, (2015)"Review of Active Power  
Decoupling Topologies in Single-Phase Systems," in IEEE Transactions on  
Power Electronics, vol. 31, no. 7, pp. 4778-4794, doi:  
10.1109/TPEL.2015.2477882.

Y. Tang and F. Blaabjerg, (2015)"A Component-Minimized Single-Phase Active  
Power Decoupling Circuit With Reduced Current Stress to Semiconductor  
Switches," in IEEE Transactions on Power Electronics, vol. 30, no. 6, pp. 2905-  
2910, doi: 10.1109/TPEL.2014.2369959.

M. A. Vitorino, R. Wang, M. B. R. Correa and D. Boroyevich, (2012)"Compensation  
of DC-link oscillation in single-phase to single-phase VSC/CSC and power

density comparison," IEEE Energy Conversion Congress and Exposition (ECCE), pp. 1121-1127, doi: 10.1109/ECCE.2012.6342692.

M. A. Vitorino, M. B. R. Correa and C. B. Jacobina, (2013)"Single-phase power compensation in a current source converter," 2013 IEEE Energy Conversion Congress and Exposition, , pp. 5288-5293, doi: 10.1109/ECCE.2013.6647417.

M. A. Vitorino, M. B. R. Correa and C. B. Jacobina, (2013)"Single-phase power compensation in a current source converter," 2013 IEEE Energy Conversion Congress and Exposition, , pp. 5288-5293, doi: 10.1109/ECCE.2013.6647417.

Huai Wang, ; Chung, Henry Shu-Hung; Wenchao Liu, (2014). Use of a Series Voltage Compensator for Reduction of the DC-Link Capacitance in a Capacitor-Supported System. IEEE Transactions on Power Electronics, 29(3), 1163–1175. doi:10.1109/TPEL.2013.2262057.

Ruxi Wang, ; Fei Wang, ; Boroyevich, D.; Burgos, R.; Rixin Lai, ; Puqi Ning, ; Rajashekara, K. (2011). [A High Power Density Single-Phase PWM Rectifier With Active Ripple Energy Storage] , 26(5), pp.1430–1443. doi:10.1109/tpel.2010.2090670.

Yilmaz, Murat; Krein, Philip T. (2013). Review of Battery Charger Topologies, Charging Power Levels, and Infrastructure for Plug-In Electric and Hybrid Vehicles. IEEE Transactions on Power Electronics, 28(5), pp.2151–2169. doi:10.1109/TPEL.2012.2212917.

Zhu, Guo-Rong; Tan, Siew-Chong; Chen, Yu; Tse, Chi K. (2013). Mitigation of Low-Frequency Current Ripple in Fuel-Cell Inverter Systems Through Waveform Control. *IEEE Transactions on Power Electronics*, 28(2), 779–792. doi:10.1109/tpel.2012.2205407.

Li, Sinan; Zhu, Guorong; Tan, Siew-Chong; Hui, S. Y. R. (2014). [IEEE 2014 IEEE Energy Conversion Congress and Exposition (ECCE) - Pittsburgh, PA, USA (2014.9.14-2014.9.18)] 2014 IEEE Energy Conversion Congress and Exposition (ECCE) - Direct AC/DC rectifier with mitigated low-frequency ripple through waveform control. , pp, 2691–2697. doi:10.1109/ECCE.2014.6953762